Response of the low ionosphere to X-ray and Lyman-a solar flare emissions

Jean-Pierre Raulin, Gérard Trottet, Matthieu Kretzschmar, Edith L. Macotela, Alessandra Pacini, Fernando Bertoni, Ingolf Dammasch

JOURNAL OF GEOPHYSICAL RESEARCH: SPACE PHYSICS, VOL. 118, 570–575, doi:10.1029/2012JA017916, 2013

Response of the low ionosphere to X-ray and Lyman-α solar flare emissions

Jean-Pierre Raulin,[1] Gérard Trottet,[2] Matthieu Kretzschmar,[3,4] Edith L. Macotela,[5] Alessandra Pacini,[6] Fernando C. P. Bertoni,[1] and Ingolf E. Dammasch[7]

Received 7 May 2012; revised 28 November 2012; accepted 2 December 2012; published 31 January 2013.

[1] Using soft X-ray measurements from detectors onboard the Geostationary Operational Environmental Satellite (GOES) and simultaneous high-cadence Lyman-α observations from the Large Yield Radiometer (LYRA) onboard the Project for On-Board Autonomy 2 (PROBA2) ESA spacecraft, we study the response of the lower part of the ionosphere, the *D* region, to seven moderate to medium-size solar flares that occurred in February and March of 2010. The ionospheric disturbances are analyzed by monitoring the resulting sub-ionospheric wave propagation anomalies detected by the South America Very Low Frequency (VLF) Network (SAVNET). We find that the ionospheric disturbances, which are characterized by changes of the VLF wave phase, do not depend on the presence of Lyman-α radiation excesses during the flares. Indeed, Lyman-α excesses associated with flares do not produce measurable phase changes. Our results are in agreement with what is expected in terms of forcing of the lower ionosphere by quiescent Lyman-α emission along the solar activity cycle. Therefore, while phase changes using the VLF technique may be a good indicator of quiescent Lyman-α variations along the solar cycle, they cannot be used to scale explosive Lyman-α emission during flares.

Citation: Raulin, J.-P., G. Trottet, M. Kretzschmar, E. L. Macotela, A. Pacini, F. C. P. Bertoni, and I. E. Dammasch (2013), Response of the low ionosphere to X-ray and Lyman-α solar flare emissions, *J. Geophys. Res. Space Physics*, *118*, 570–575, doi:10.1029/2012JA017916.

1. Introduction

[2] The Lyman-α radiation of solar chromospheric origin at 121.6 nm belongs to the vacuum ultraviolet spectral range and is by far the most intense line in the solar irradiance spectrum. It is only because of the low absorption cross-section of molecular oxygen (O_2) at about $\leq 10^{-21}$–10^{-20} cm^2 that the Lyman-α radiation can penetrate into the mesosphere down to the 70–75 km altitude range, where it is also the main agent in the direct ionization of NO [*Nicolet and Aikin*, 1960; *Kockarts*, 2002], responsible for the formation of the *D* region. For these reasons, the solar Lyman-α radiation is an important factor for the dynamics of the atmosphere at these altitudes, resulting in molecular oxygen and water-clusters dissociation and participating actively in the distribution of minor species such as water vapor, ozone, and nitric oxide [*Woods et al*., 2000 and references therein]. However, only sparse space measurements exist, and adjustments between them have been achieved through important modeling efforts using proxies, like SOLAR2000 [*Tobiska et al*., 2000], in order to infer Lyman-α variations on long timescales. A suitable alternative is the monitoring and analysis of very low frequency (VLF; 3–30 kHz) wave propagation anomalies. VLF waves propagate by multiple reflections over long distances within the Earth-ionosphere waveguide, and their phase and amplitude provide information about the electrical properties of the waveguide's conducting boundaries, i.e., the reference height *H* and the conductivity gradient β of the Earth's surface and of the low ionospheric plasma of the *D* region [*Wait*, 1959; *Wait and Spies*, 1964].

[3] Sub-ionospheric propagating VLF waves have been used to study external forcing agents like solar flare X-rays [*Bracewell and Straker*, 1949; *Comarmond*, 1977; *Muraoka et al*., 1977; *Thomson et al*., 2005; *Raulin et al*., 2010], γ-ray bursts from astrophysical remote objects [*Tanaka et al*., 2010], or meteor showers [*Chilton*, 1961; *Kaufmann et al*., 1989]. During solar flares, it has been shown that only soft X-ray photons with $\lambda < 2$ Å can penetrate down to 70 km altitude and lower [*Pacini and Raulin*, 2006] and produce significant ionization enhancements that result in variations of one or both of the Wait parameters. On longer timescales,

[1]Centro de Radio Astronomia e Astrofísica Mackenzie, CRAAM, Universidade Presbiteriana Mackenzie, São Paulo, SP, Brazil.
[2]Observatoire de Paris, LESIA-CNRS UMR 8109, Univ. P & M Curie and Paris-Diderot, Observatoire de Meudon, Meudon, France.
[3]Solar Terrestrial Center of Excellence, Royal Observatory of Belgium, Brussels, Belgium.
[4]LPC2E, UMR 6116 CNRS & University of Orléans, Orléans, France.
[5]Comisión Nacional de Investigación y Desarrollo Aeroespacial (CONIDA), Lima, Peru.
[6]Universidade do Vale do Paraíba (UNIVAP), São José dos Campos, SP, Brazil.
[7]Solar Influence Data Analysis Center/Royal Observatory of Belgium, Brussels, Belgium.

Corresponding author: Jean-Pierre Raulin, Centro de Radio Astronomia e Astrofísica Mackenzie, CRAAM, Universidade Presbiteriana Mackenzie, São Paulo, SP, Brazil. (raulin@craam.mackenzie.br)

2169-9380/13/2012JA017916

the variability of the quiescent Lyman-α emission between solar minimum and maximum has been proposed to account for the differences of the observed ionospheric response to solar flares [*Pacini*, 2006; *Pacini and Raulin*, 2006]. The same Lyman-α variability was also found to be responsible for the long-term changes of the properties of the ionospheric *C* region [*Raulin et al*., 2011].

[4] It is only recently that continuous high-cadence (50 ms) observations of the Lyman-α solar irradiance have been obtained by the PROBA2/LYRA (Project for On-Board Autonomy 2/Large Yield Radiometer) radiometer. This provides a unique opportunity to measure the short-term Lyman-α variability and look for its eventual effect on the low ionosphere. In this paper, we use LYRA and South America VLF Network (SAVNET) capabilities to compare the ionospheric response to moderate and medium-size solar flares and look for differences depending on whether or not the flare was accompanied by transient Lyman-α excesses. In the next section, we report on the instrumentation used and the method for data analysis. Our results are presented and discussed in section 3, and concluding remarks are given in section 4.

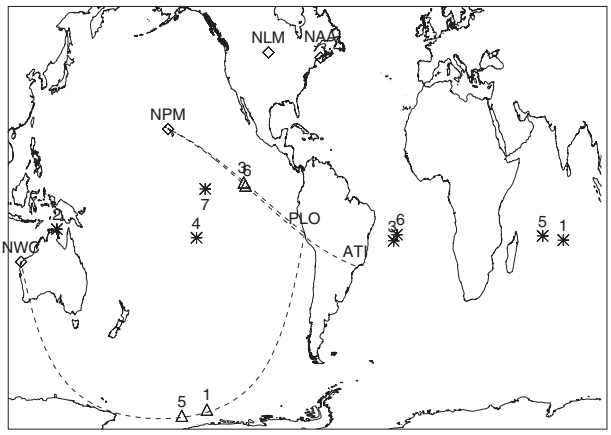

Figure 1. Map showing the VLF wave propagation paths NWC-PLO, NPM-PLO, and NPM-ATI between transmitters NPM (21.4 kHz) and NWC (19.8 kHz) and receivers PLO (Punta Lobos, Peru) and ATI (Atibaia, Brazil). Star symbols indicate the sub-flare point for each of the events. Triangle symbols indicate the location where the terminator crosses the VLF propagation path for the flares during which the path was not totally illuminated (1, 3, 5, 6).

2. Instrumentation and Data Analysis

[5] The SAVNET array is currently composed of nine VLF tracking stations located in Brazil, Peru, Argentina, and Mexico. Few additional receivers will be installed sometime in 2012 in Northern Brazil and Eastern Europe. SAVNET is used to study VLF wave propagation anomalies due to external disturbances, like solar flares, solar activity phenomena, and γ-ray bursts from astrophysical remote objects [*Raulin et al*., 2006; *Tanaka et al*., 2010; *Raulin et al*., 2011] or induced from below the lower ionosphere like planetary waves [*Correia et al*., 2011] and seismic electromagnetic effects [*Hayakawa et al*., 2011]. Each receiver is composed of three electromagnetic sensors, and the VLF signals received from powerful transmitters are amplified and then digitized using a commercial audio card. The measured output parameters are the phase and amplitude of the transmitted VLF wave. The received amplitude depends on the integrated absorption of the wave at all distances along the propagation path and at all altitudes below the reflection height, while the received phase is mainly dependent on the reflection height [*Watt*, 1967]. In this paper, we then focus on phase advances only. The sensitivity of the phase measurements is set by the RMS noise in the phase data and will depend on the conditions of wave propagation and thus on the chosen propagation path. Adopting a 3 × RMS criteria, the lower sensitivity for a 1 s time constant is of the order of 2 degrees. Further details on the SAVNET receiver locations, instrumental setup, and scientific goals are described in *Raulin et al*. [2009, 2010].

[6] In order to have a uniform set of phase advance measurements, when possible, we have chosen VLF paths with similar orientations between the transmitter and the receiver and similar wave propagation directions. In Figure 1, we show the three VLF propagation paths used between transmitters NPM (Lulalai, Hawaii, 21.4 kHz) and NWC (NorthWest Cape, Australia, 19.8 kHz) and receivers PLO (Punta Lobos, Peru) and ATI (Atibaia, Brazil). The VLF path used for each event is also indicated in Table 1 (see section 3). Figure 1 indicates that all three VLF propagation paths are west-east oriented, with a wave propagation direction from west to east. In order to check how our results depend on the path orientation, other transmitters are available such as NLM (La Moure, North Dakota, US, 25.2 kHz) and NAA (Cutler, Maine, USA, 24.0 kHz). Moreover, except for the path NPM-ATI which is located above land for ~25% of its length, Figure 1 shows that wave propagation is essentially over sea, limiting the effects of higher mode propagation.

Table 1. Data on the Studied Events[a]

Date, Time	VLF Path	GOES Max. Flux (10^{-6} W/m^2)	LYMAN-α (Y/N), (10^{-5} W/m^2)	F_{tot} (10^{-5} J/m^2)	ΔΦ (Deg.)
Feb 6 2010, 0705 UT (1)	NWC-PLO	4.0	Y, 1.2	3.47	16.7 ± 6
Feb 7 2010, 2115 UT (2)	NPM-PLO	4.2	Y, 2.0	2.34	13.3 ± 2
Feb 8 2010, 1347 UT (3)	NPM-PLO	20.0	Y, 4.55	37.8	47.2 ± 3
Feb 7 2010, 2140 UT (4)	NPM-PLO	4.2	N, <0.15	3.64	19.0 ± 2
Feb 13 2010, 0752 UT (5)	NWC-PLO	4.3	N, <0.12	3.04	17.4 ± 5
Feb 13 2010, 1240 UT (6)	NPM-ATI	9.6	N, <0.09	17.16	33.3 ± 2
Mar 26 2010, 2110 UT (7)	NPM-PLO	2.5	N, <0.1	1.40	7.9 ± 3

[a]From left to right, the different columns indicate the following for each studied event: the date, time, and event number; the VLF propagation path considered; the X-ray peak flux; whether (Y) or not (N) the event is associated with an excess of the Lyman-α flux and the value of this excess; the total X-ray fluence, F_{tot}; and the normalized phase variation ΔΦ and its 3 RMS uncertainty.

[7] The treatment of the phase data was done as follows. The phase advances ΔΦ are first normalized to the length of the sunlit path. For the events studied here, the illuminated portion of the propagation paths is long enough (>3000 km) so that the effects of higher propagating modes on the received phase should be negligible. Then, for each event, a mean solar zenith angle, χ, was estimated along the sunlit path at the time of the maximum phase advance. To achieve this, each VLF propagation path is divided into 500 parts; a solar zenith angle χ_i (i = 1, 500) is computed for each of the illuminated pieces, and χ is taken as the mean of the χ_i. In order to take into account the solar illumination conditions as in *Muraoka et al*. [1977], the phase advances are corrected by the factor $[\cos(\chi)]^{-1}$. Finally, the values of ΔΦ were normalized to a distance of 2.88 Mm in order to compare our results with those of *Pacini and Raulin* [2006]. For paths with similar directions (here EW), the above procedure allows estimation of ΔΦ values which are not critically dependent of the VLF propagation path length and of its illumination conditions. Indeed, using NPM-ATI (length of 13.07 Mm) and NPM-PLO (length of 9.65 Mm) for a given flare, we obtain ΔΦ values which differ by less than 1 degree, that is, smaller than the uncertainties given in Table 1. However, for the flares studied here, ΔΦ values obtained by considering NS propagation paths between transmitters NAA (24.0 kHz) and NLM (25.2 kHz) and receivers PLO and ATI are up to 7 degrees larger than those obtained by considering EW oriented paths.

[8] The solar flare X-ray database used in this paper is composed of soft X-ray fluxes measured by the Geostationary Operational Environmental Satellite (GOES) detectors which record solar photons in the 1–8 and 0.5–4 Å wavelength channels (NOAA, Space Weather Prediction Center), corresponding to photon energies in the range 2–12 keV. We are interested in X-ray photons with $\lambda < 2$ Å (see section 1) because higher wavelength photons are mainly absorbed above 80 km of altitude and do not disturb the *D* region [*Pacini and Raulin*, 2006; *Satori et al*., 2005]. Therefore, fluences integrated over the 0.5–2 Å wavelength range have been computed in the same way as in *Pacini and Raulin* [2006]. Namely, we assume that X-rays are emitted by the hot isothermal plasma associated with the flaring active region. Then the temperature, $T(t)$, and emission measure, EM(t), of the emitting plasma are derived as a function of time, t, using the two wavelength channels of the GOES detectors, and the Mewe abundance and ionization equilibrium models [*Mewe et al*., 1985]. Using $T(t)$ and EM(t), we calculate the isothermal spectrum of the source as a function of the photon wavelength for each time t and integrate it between 0.5 and 2 Å in order to get the instantaneous X-ray flux within this wavelength range, $F(t)$. It should be noted that the use of CHIANTI models with coronal elemental abundances [*Landi et al*., 1999, 2002] are in principle more appropriate than Mewe models for hot flaring plasma. Nevertheless, we stayed with Mewe models in order to obtain fluence values derived in the same way as those reported in previous works [e.g., *Pacini and Raulin*, 2006]. While the instantaneous flux of the incoming X-rays, $F(t)$, is related to the ionization rate in the low ionosphere, the net VLF phase changes, ΔΦ, reflect an energy deposit which is related to the fluence, F_{tot}, obtained by integrating, $F(t)$ between the start of the soft X-ray emission and the peak of the VLF phase advance [e.g., *Pacini and Raulin*, 2006].

[9] The LYRA [*Hochedez et al*., 2006; *Dominique et al*., 2012] instrument monitors the solar irradiance at very high cadence (50 ms nominally) in four ultraviolet channels, one of which is dedicated to the strong Lyman-α line at 121.6 nm. The radiometer is onboard the PROBA2 spacecraft (ESA) and started its operation on 6 January 2010. The nominal LYRA Lyman-α channel experienced strong degradation early in the mission but recorded several M- and C-class flares in February and March 2010, some having a clear signature in the Sun-integrated Lyman-α light (and other not). For the events studied here, we started with the (uncalibrated) LYRA level 1 data and processed them following *Kretzschmar et al*. [2012] in order to remove effects that can affect the flare signal; in more details, we (1) removed a dark current excess that is observed during some periods early in the PROBA2 missions, (2) corrected for the LYRA channel degradation with a multiplicative factor, and (3) used the absolute value given by the Solar Radiation and Climate Experiment (SORCE)/Solar Stellar Irradiance Comparison Experiment (SOLSTICE) instrument for that day to convert count rates in physical units. These steps allow a better estimate of the true Lyman-α excess during flare than by using the calibrated LYRA level 2 data directly. The PROBA2 spacecraft suffers a large angle rotation (LAR) approximately every 25 min, creating sharp dips and peaks in the Lyman-α time profile. Thus, flares occurring close to a LAR have not been considered.

3. Observational Results and Discussion

[10] Figure 2 shows the time evolution of $F(t)$ (top), of the background subtracted Lyman-α emission (middle), and of ΔΦ(t) (bottom) for a flare associated with a significant excess of Lyman-α radiation (left) and a flare without measurable excess of Lyman-α radiation (right). As explained in Section 2, each ΔΦ has been corrected for the corresponding mean solar zenith angle χ and normalized to an illuminated distance of 2.88 Mm. The vertical dashed line on the left indicates the onset time of the soft X-ray emission (3σ over background) in the 1–8 Å channel, while the vertical dashed line on the right indicates the time of the maximum VLF phase advance. The quantity defined in section 2, F_{tot}, has been obtained by integrating $F(t)$ between these two times. The events in Figure 2 correspond to two flares with similar F_{tot} and ΔΦ values, although only one of them exhibits Lyman-α excess emission. The 7 February 2010 flare started during the decreasing part of an earlier event which is not shown since it occurred close to a LAR of the PROBA2 spacecraft.

[11] Table 1 displays the date and time, the event number, the VLF path used, the GOES peak flux, F_{tot} and the VLF maximum phase advance for the seven solar events of moderate to medium sizes (GOES class from C2.5 to M2.0) studied in this paper. It also indicates if a given flare is associated with a Lyman-α excess (Y) or not (N), the Lyman-α excess if it is significant, and the RMS noise otherwise. It should be noted that, when significant, the Lyman-α excesses remain ≤1% of the quiescent pre-flare background level.

[12] Figure 3 shows ΔΦ as a function of F_{tot} for the seven solar events under study. Three were associated with significant Lyman-α excesses (squares), and the other four were not (triangles). For each event, the fluence error bars represent

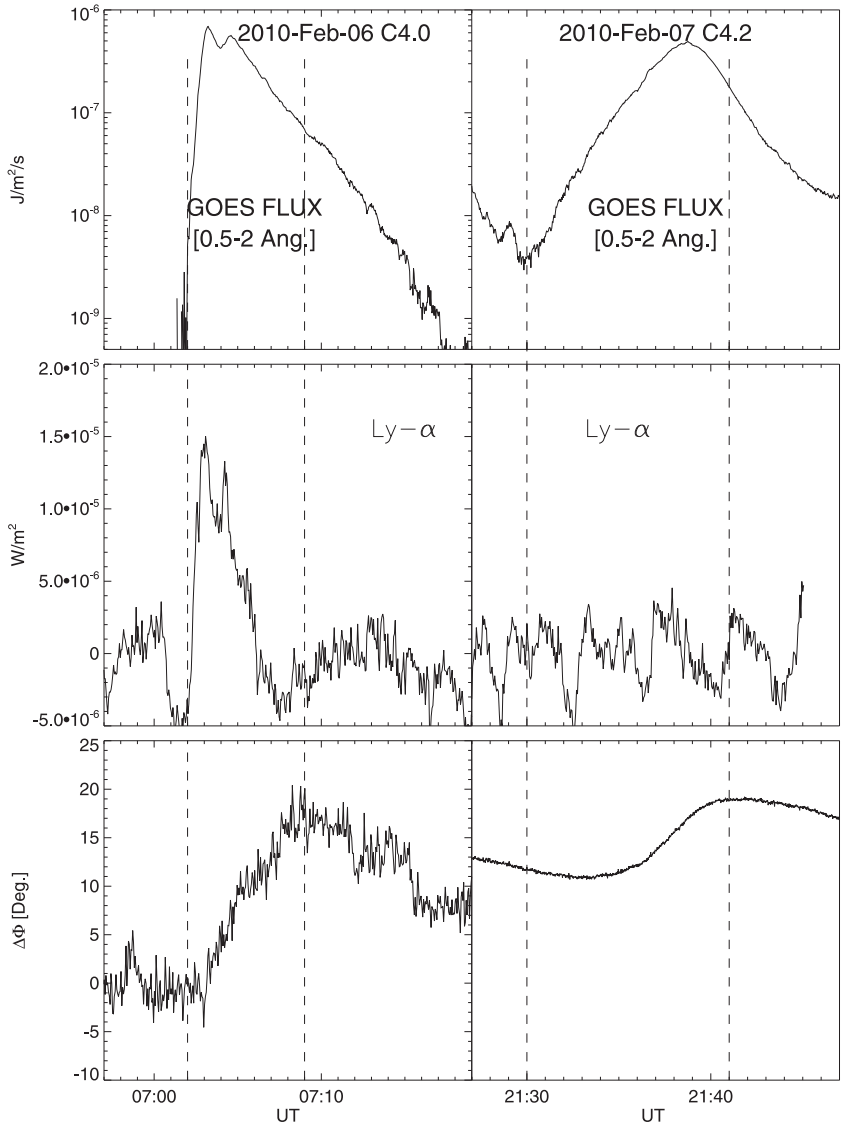

Figure 2. Time evolution of the X-ray (0.5–2 Å) flux $F(t)$ (top), of the Lyman-α excess (middle), and of the VLF phase advance ΔΦ (bottom) observed during a solar flare with (left) and without (right) significant excess of Lyman-α emission. The dashed lines show the start time of the soft X-ray emission detected by GOES in the 1–8 Å channel and the peak time of ΔΦ. Vertical scales are the same for both displayed events.

the spread of the F_{tot} values calculated with and without background subtraction. Error bars for ΔΦ (full vertical lines) are sized to three times the RMS variation of the phase data as indicated in the last column of Table 1. The crosses at the top of the vertical dashed lines show the values of ΔΦ obtained using NS oriented propagation paths (see section 2), when possible. The dash-dotted lines in Figure 3 show the variations of ΔΦ (for a VLF propagation path of 2.88 Mm length) as a function of F_{tot} inferred by *Pacini and Raulin* [2006] for solar flares occurring around solar minimum (upper dashed line) and around solar maximum (lower dashed line).

[13] From Figures 2 and 3 and Table 1, we remark the following:

[14] • Some solar flares are clearly associated with excesses of Lyman-α radiation, and others are not, independently of their X-ray peak flux; all the studied events do present a VLF phase advance within the range of values inferred by *Pacini and Raulin* [2006] for flares occurring during solar minimum and during maximum periods; Figure 3 shows that this finding is independent of the orientation of the VLF propagation path.

[15] • For the three events of similar X-ray fluence, there is no significant difference between the observed ΔΦs whether they are associated with Lyman-α excesses (event 1) or not (events 4 and 5). This conclusion is only valid for flare-associated VLF effects measured with similar orientation path (see section 2).

[16] The above results indicate that the ionospheric effect of Lyman-α radiation associated with flares is negligible compared to that produced by soft X-rays. This statement is consistent with the fact that the observed Lyman-α flux excesses are about only [0.3–1]% of the background value.

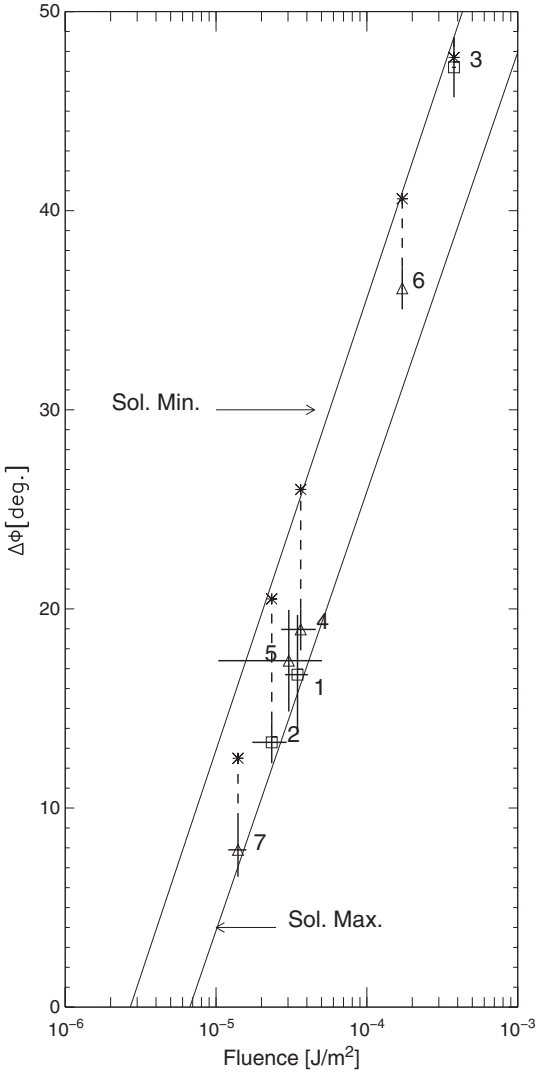

Figure 3. The VLF phase changes ΔΦ as a function of the X-ray fluence F_{tot} during the seven solar flares under study. Squares and triangles represent respectively solar events with and without associated excesses of Lyman-α emission. The upper and lower dash-dotted lines are the ΔΦ values inferred for flares occurring close to solar minimum and to solar maximum, respectively [*Pacini and Raulin*, 2006]. The crosses at the top of the vertical dashed lines show the values of ΔΦ obtained using NS oriented propagation paths.

This can be understood, for example, if the flaring radiation in Lyman-α, which comes from localized regions of the solar disk, is too small, compared with the quiescent emission originating from the whole disk, to produce significant ΔΦ.

[17] *Raulin et al*. [2006] and *Pacini and Raulin* [2006] indicate that the response of the ionospheric *D* region, when disturbed by a given solar flare, is stronger during solar minimum than during solar maximum. Their interpretation is that the quiescent ionospheric reference height is higher for solar minimum conditions than for solar maximum. This change of the reference height is attributed to the variation of the quiescent Lyman-α irradiance through the solar activity cycle. This conclusion is in agreement with simulations of VLF wave propagation performed by *McRae and Thomson* [2000; 2004] to estimate the *D* region altitude. For solar cycle 22, *Pacini and Raulin* [2006] have shown that ΔΦ changes by 10 degrees. This corresponds to a decrease of the reference height by 1 km.

[18] The composite Lyman-α time series from 1947 to the actual epoch [*Woods et al*., 2000] includes measurements and modeling results, and from 2003 to the present time it is composed of measurements from the Thermosphere Ionosphere Mesophere Energetics and Dynamics (TIMED) and SORCE space missions [*Woods et al*., 2005; *Rottman et al*., 2006]. The expected increase of the quiescent Lyman-α emission during solar maximum is about 2.2×10^{11} photons/cm^2/s, or equivalently 3.64×10^{-3} W/m^2. This corresponds to a 60% increase of the quiescent Lyman-α level and a 10 degree increase in ΔΦ. Consequently, the Lyman-α flaring excesses reported in Table 1 in the range $[1.2–4.55] \times 10^{-5}$ W/m^2 would produce phase variations in the interval ΔΦ~[0.03–0.1] degrees. This is well below the sensitivity of VLF phase measurements. Even if LYRA can underestimate the Lyman-α flare emission by a factor 10, this would remain too small to be measured.

[19] It would be relevant to understand why some X-ray solar flares are accompanied by Lyman-α radiation excesses while others are not. This question deserves further investigation and is beyond the scope of this paper. However, we remark that while soft X-rays result from the heating of coronal regions in response to the primary flare energy release process, the Lyman-α radiation most likely results from the transport of part of this energy from the corona to the chromosphere and its deposition there. As transport conditions may vary from flare to flare, a strong correlation between the X-ray flux and the level of flare associated Lyman-α radiation is not necessarily expected.

4. Concluding Remarks

[20] By comparing the response of the lower ionosphere to seven solar flares of moderate to medium sizes, we have shown that the impact of transient solar Lyman-α excesses on the electrical conductivity of the *D* region is negligible. According to our estimates, the observed Lyman-α excesses during the studied solar flares represent only a very small fraction (<1%) of the background emission. This is consistent with the fact that Lyman-α flaring regions are small compared to the full solar disk which radiates the quiescent Lyman-α radiation. In terms of VLF phase measurements, the Lyman-α flare excesses reported here are estimated to produce phase changes about 20 times below the sensitivity of the present VLF measurements. Thus, although the quiescent solar Lyman-α radiation can be monitored along the solar cycle using the VLF technique, the explosive excesses observed in Lyman-α cannot. Their impacts in the low ionosphere are indeed well below the VLF sensitivity detection limit.

[21] **Acknowledgments.** J.P.R. would like to thank funding agencies MACKPESQUISA and CNPq (Proc. 305655/2010-8), as well as the Observatoire de Paris for funding a 1 month stay in January 2012 during which part of this work was developed. F.C.P.B. thanks FAPESP (Proc. 2007/05630-1). The SAVNET project was funded by FAPESP (Proc. 06/02979) and received partial funds from CNPq (482000/2011-2) and Centre National de la Recherche Scientifique (CNRS). The contribution of M.K. has been supported by the European Community's Seventh Framework Programme (FP7/2007-2013) under the grant agreement n° 261948 (ATMOP project, www.atmop.eu).

References

Bracewell, R. N., and T. W. Straker (1949), The study of solar flares by means of very long radio waves, *Mon. Not. R. Astron. Soc.*, *109*, 28–45.

Comarmond, J.-M. (1977), Contribution à l'étude de la basse ionosphère par des mesures de phase et d'amplitude d'ondes électromagnétiques à très basse fréquence, Thèse de Doctorat d' Etat, Université Pierre et Marie Curie, Paris VI.

Correia, E., P. Kaufmann, J.-P. Raulin, F. C. P. Bertoni, and H. R. Gavilán (2011), Analysis of daytime ionosphere behavior between 2004 and 2008 in Antarctica, *J. Atmos. Sol. Terr. Phys.*, *73*, 2272–2278.

Chilton, C. J. (1961) VLF phase perturbation associated with meteor shower ionization, *J. Geophys. Res.* , *66*, 379–383.

Dominique, M., et al. (2012), The LYRA instrument onboard PROBA2: Description and in-flight performance, submitted to *Solar Physics*.

Hayakawa, M., J.-P. Raulin, Y. Kasahara, F. C. P. Bertoni, Y. Hobara, and W. Guevara-Day (2011), Ionospheric perturbations in possible association with the 2010 Haiti earthquake, as based on medium-distance subionospheric VLF propagation data, *Nat. Hazard. Earth Syst. Sci.*, *11*, 513–518.

Hochedez, J.-F., et al. (2006), LYRA, a solar UV radiometer on PROBA2, *Adv. Space Res. 37*, 303–312.

Kaufmann, P., V. L. R. Kuntz, N. M. Paes Leme, L. R. Piazza, and J. W. S. Vilas Boas (1989), Effects of the large June 1975 meteoroid storm on Earth's ionosphere, *Science*, *246*, 787–790.

Kockarts, G. (2002), Aeronomy, a 20th century emergent science: The role of solar Lyman series, *Ann. Geophys.*, *20*, 585–598.

Kretzschmar, M., M. Dominique, and I. E Dammasch (2012), Sun-as-a-star observation of flares in Lyman-α by the PROBA2/LYRA radiometer, *Sol. Phys.*, doi:10.1007/s11207-012-0175-610.

Landi, E., U. Feldman, and K. P. Dere (2002), CHIANTI—An atomic database for emission lines. V. Comparison with an isothermal spectrum observed with SUMER, *Astrophys. J. Suppl.*, *139*, 281–296.

Landi, E., M. Landini, K. P. Dere, P. R. Young, and H. E. Mason (1999), CHIANTI—An atomic database for emission lines. III. Continuum radiation and extension of the ion database, *Astron. Astrophys. Suppl. Ser.*, *135*, 339–346.

McRae, W. W., and N. R. Thomson (2000), VLF phase and amplitude: Daytime ionospheric parameters, *J. Atmos. Sol. Terr. Phys.*, *62*, 609–618.

McRae, W. M., and N. R. Thomson (2004), Solar flare induced ionospheric *D*-region enhancements from VLF phase and amplitude observations, *J. Atmos. Sol. Terr. Phys.*, *66*, 77–87.

Mewe, R., E. H. B. M. Gronenschild, and G. H. J. van den Oord (1985), Calculated X-radiation from optically thin plasma, *Astron. Astrophys., Suppl.*, *62*, 197–254.

Muraoka, Y., H. Murata, and T. Sato (1977), The quantitative relationship between VLF phase deviations and 1–8 Å solar X-ray fluxes during solar flares, *J. Atmos. Terr. Phys.*, *39*, 787–792.

Nicolet, M., and A. C. Aikin (1960), The formation of the *D*-region of the ionosphere, *J. Geophys. Res.*, *65*, 1469–1483.

Pacini, A. A. (2006), Dependência das propriedades da região-D ionosférica com o ciclo de atividade solar, Dissertação de Mestrado em Geofísica Espacial, INPE, São José dos Campos.

Pacini, A. A., and J.-P. Raulin (2006), Solar X-ray flares and ionospheric sudden phase anomalies relationship: A solar cycle phase dependence, *J. Geophys. Res.*, *111*, A09301, doi:10.1029/2006JA011613.

Raulin, J.-P., A. A. Pacini, P. Kaufmann, E. Correia, and M. A. G. Martinez (2006), On the detectability of solar X-ray flares using very low frequency sudden phase anomalies, *J. Atmos. Sol. Terr. Phys.*, *68*, 1029–1035.

Raulin, J.-P., P. David, R. Hadano, A. C. V. Saraiva, E. Correia, and P. Kaufmann (2009), The South America VLF NETwork (SAVNET), *Earth, Moon and Planets*, *104*, 247–261.

Raulin, J.-P., et al. (2010), Solar flare detection sensitivity using the South America VLF Network (SAVNET), *J. Geophys. Res.*, *115*, A07301, doi:10.1029/2009JA015154.

Raulin, J.-P., F. C. P. Bertoni, P. Kaufmann, H. R. Gavilán, E. Correia, R. Hadano, and N. J. Schuch (2011), Solar-Terrestrial, ionospheric and natural phenomena studies using the South America VLF Network (SAVNET), *J. Atmos. Sol. Terr. Phys.*, *73*, 1581–1586.

Rottman, G. J., T. N. Woods, and W. McClintock (2006), SORCE solar UV irradiance results, *Adv. Space Res.*, *37*, 201–208, doi: 10.1016/j.asr.2005.02.072.

Sátori, G., E. Williams, and V. Mushtak (2005), Response of the Earth ionosphere cavity resonator to the 11-year solar cycle in X-radiation, *J. Atmos. Sol. Terr. Phys.*, *67*, 553–562.

Tanaka, Y. T., J.-P. Raulin, F. C. P. Bertoni, P. R. Fagundes, J. Chau, N. J. Schuch, Y. Hobara, T. Terasawa, and T. Takahashi (2010), First very low frequency detection of short repeated bursts from Magnetar SGR J1550-5418, *Astrophys J. Lett.*,*721*, L24–L27.

Thomson, N. R., C. J. Rodger, and M. A. Clilverd (2005), Large solar flares and their ionospheric *D*-region enhancements, *J. Geophys. Res.*, *110*(A6), A06306–A06316.

Tobiska, W. K., T. Woods, F. Eparvier, R. Viereck, L. Floyd, D. Bouwer, G. Rottman, and O. R. White (2000), The SOLAR2000 empirical solar irradiance model and forecast tool, *JASTP*, *62*, 1233–1250.

Wait, J. R. (1959), Diurnal change of ionospheric heights deduced from phase velocity measurements at VLF, Proc. *IRE*, *47*, 998.

Wait, J. R., and K. Spies (1964), Characteristics of the Earth-ionosphere waveguide for VLF radio waves, NBS Technical NoteU.S., 300.

Watt, A. D. (1967), V. L. F. Radio Engineering, International Series of Monograph in Electromagnetic Waves, Pergamon Press, Glasgow, Chapter III.

Woods, T. N., W. K. Tobiska, G. J. Rottman, and J. R. Worden (2000), Improved solar Lyman α irradiance modeling from 1947 through 1999 based on UARS observations, *J. Geophys. Res.*, *105*, 27195–27215.

Woods, T. N., F. G. Eparvier, S. M. Bailey, P. C. Chamberlin, J. Lean, G. J. Rottman, S. C. Solomon, W. K. Tobiska, and D. L. Woodraska (2005) The Solar EUV Experiment (SEE): Mission overview and first results, *J. Geophys. Res.*, *110*, A01312, doi:10.1029/2004JA010765.